Supplementary Material for:

Simplified tuning of long-range corrected time-dependent density functional theory

Aniket Mandal and John M. Herbert*
Department of Chemistry and Biochemistry
The Ohio State University, Columbus, Ohio 43210 USA

February 23, 2025

Contents

List of Tables

List of Figures

*herbert@chemistry.ohio-state.edu

References

[1] Peach, M. J. G.; Benfield, P.; Helgaker, T.; Tozer, D. J. Excitation energies in density functional theory: An evaluation and a diagnostic test. *J. Chem. Phys.* **2008,** *128,* 044118:1–18.

[2] Herbert, J. M.; Jacobson, L. D. Structure of the aqueous electron: Assessment of one-electron pseudopotential models in comparison to experimental data and time-dependent density functional theory. *J. Phys. Chem. A* **2011,** *115,* 14470–14483.

[3] Uhlig, F.; Herbert, J. M.; Coons, M. P.; Jungwirth, P. Optical spectroscopy of the bulk and interfacial hydrated electron from ab initio calculations. *J. Phys. Chem. A* **2014,** *118,* 7507–7515.

[4] Carter-Fenk, K.; Mundy, C. J.; Herbert, J. M. Natural charge-transfer analysis: Eliminating spurious charge-transfer states in time-dependent density functional theory via diabatization, with application to projection-based embedding. *J. Chem. Theory Comput.* **2021,** *17,* 4195–4210.

[5] Carter-Fenk, K.; Johnson, B. A.; Herbert, J. M.; Schenter, G. K.; Mundy, C. J. Birth of the hydrated electron via charge-transfer-to-solvent excitation of aqueous iodide. *J. Phys. Chem. Lett.* **2023,** *14,* 870–878 Erratum: *J. Phys. Chem. Lett.* **14**, 4150 (2023).

[6] Loos, P.-F.; Comin, M.; Blase, X.; Jacquemin, D. Reference energies for intramolecular charge-transfer excitations. *J. Chem. Theory Comput.* **2021,** *17,* 3666–3686.

[7] Grimme, S.; Parac, M. Substantial errors from time-dependent density functional theory for the calculation of excited states of large π systems. *ChemPhysChem* **2003,** *4,* 292–295.

[8] Loos, P.-F.; Scemama, A.; Boggio-Pasqua, M.; Jacquemin, D. Mountaineering strategy to excited states: Highly accurate energies and benchmarks for exotic molecules and radicals. *J. Chem. Theory Comput.* **2020,** *16,* 3720–3736.

TABLES

Table S1: CT excitation energy data set.

Molecule	State	Benchmark[a] (eV)	ω (bohr^{-1})[b]		TD-DFT Errors (eV)[c]					
			GDD	IE	LRC-ω_{GDD}PBE	LRC-ω_{IE}PBE	B3LYP	PBE0	CAM-B3LYP	LRC-ωPBEh
Aminobenzonitrile	$2\,^1A_1$	5.26	0.314	0.293	−0.09	0.12	−0.35	−0.25	−0.15	−0.22
Aniline	$2\,^1A_1$	5.87	0.324	0.305	−0.21	−0.02	−0.45	−0.35	−0.30	−0.22
Azulene	$2\,^1A_1$	3.89	0.300	0.241	−0.11	−0.17	−0.28	−0.21	−0.16	0.06
Azulene	$^1B_2$	4.55	0.300	0.241	0.21	0.13	0.08	0.17	0.22	0.08
Benzonitrile	$^1A_1$	7.10	0.328	0.297	−0.34	−0.41	−0.90	−0.80	−0.50	0.00
Benzothiadiazole	$^1B_2$	4.37	0.312	0.443	−0.08	0.06	−0.58	−0.47	−0.26	−0.16
Dimethylaniline	$^1B_2$	4.47	0.305	0.266	0.20	0.12	−0.04	0.05	0.22	0.07
Dimethylaniline	$^1A_1$	5.54	0.305	0.266	−0.04	−0.10	−0.42	−0.20	−0.08	0.05
Nitroaniline	$^1A_1$	4.57	0.320	0.284	−0.08	−0.13	−0.64	−0.49	−0.21	0.04
Nitrodimethylaniline	$^1A_1$	4.28	0.307	0.248	0.02	−0.15	−0.61	−0.46	−0.14	0.16
Phthalazine	$^1A_2$	3.93	0.312	0.275	0.01	−0.15	−0.41	−0.28	0.12	0.11
Phthalazine	$^1B_1$	4.34	0.312	0.275	0.46	0.41	−0.40	−0.29	0.05	0.04
Quinoxaline	$^1B_2$	4.74	0.311	0.341	−0.04	0.04	−0.65	−0.53	−0.23	−0.11
Quinoxaline	$^1A_1$	5.75	0.311	0.341	0.22	0.27	−0.03	0.08	0.18	−0.07
Quinoxaline	$^1B_1$	6.33	0.311	0.341	0.05	0.10	−0.41	−0.45	−0.11	−0.07
Twisted DMABN	$^1A_2$	4.17	0.303	0.279	−0.23	−0.36	−0.96	−0.83	−0.19	0.12
Twisted DMABN	$^1B_1$	4.84	0.303	0.279	0.37	0.33	−0.97	−0.80	−0.11	0.02
Dipeptide	$n_1 \rightarrow \pi_2^*$	8.07	0.317	0.325	−0.24	−0.08	−1.84	−1.51	−0.27	−0.26
Dipeptide	$\pi_1 \rightarrow \pi_2^*$	7.18	0.317	0.325	0.02	0.05	−1.10	−0.86	−0.30	−0.09
β-dipeptide	$n_1 \rightarrow \pi_2^*$	9.13	0.307	0.296	−0.24	0.15	−1.87	−1.49	−0.75	−0.43
β-dipeptide	$\pi_1 \rightarrow \pi_2^*$	7.99	0.307	0.296	−0.33	0.01	−0.79	−0.17	0.02	−0.40
N-phenylpyrrole	$2\,^1B_2$	5.47	0.312	0.464	−0.03	0.25	−0.86	−0.71	−0.20	−0.07
N-phenylpyrrole	$3\,^1A_1$	5.94	0.312	0.464	0.39	0.71	−1.29	−1.13	−0.02	−0.08
DMABN	^1A	4.56	0.314	0.257	0.35	0.33	0.01	0.11	0.27	0.12

[a]From Refs. 1 and 6. [b]LRC-ωPBE/def2-TZVPD. [c]TD-DFT/def2-TZVPD, full linear response (no TDA). Positive errors indicate that the TD-DFT transition energy is larger than the benchmark value.

Table S2: Valence excitation energy data set, from Ref. 1.

Molecule	State	TD-DFT Errors (eV)[a]						Benchmark[b] (eV)
		LRC-ω_{GDD}PBE	LRC-ω_{IE}PBE	PBE	PBE0	HF-PBE	CIS	
Dipeptide	$n_1 \rightarrow \pi_1^*$	−0.05	−0.03	−0.28	−0.02	0.95	1.10	5.62
Dipeptide	$n_2 \rightarrow \pi_2^*$	0.00	0.02	−0.14	0.02	1.00	1.14	5.79
β-Dipeptide	$n_1 \rightarrow \pi_1^*$	0.13	0.27	−0.05	0.27	1.20	1.35	5.40
β-Dipeptide	$n_2 \rightarrow \pi_2^*$	0.51	0.50	0.33	0.49	1.47	1.63	5.10
Naphthalene	$^1B_{2u}$	−0.11	−0.21	−0.77	−0.41	−0.05	0.18	4.88
Naphthalene	$^1B_{3u}$	0.13	0.07	−0.19	0.09	0.58	0.75	4.46
Anthracene	$^1B_{2u}$	−0.06	−0.20	−0.77	−0.42	0.09	0.98	3.69
Anthracene	$^1B_{3u}$	0.12	0.03	−0.26	0.05	0.51	0.71	3.89
Tetracene	$^1B_{2u}$	−0.04	0.13	−0.74	−0.41	0.10	1.41	2.90
Tetracene	$^1B_{3u}$	0.11	0.11	0.05	0.01	0.43	0.66	3.52
Pentacene	$^1B_{2u}$	−0.03	−0.14	−0.73	−0.41	0.07	0.40	2.35
Pentacene	$^1B_{3u}$	0.11	0.06	−0.89	−0.19	0.36	1.35	3.27
Hexacene	$^1B_{2u}$	0.14	−0.07	−0.72	−0.42	0.03	0.38	1.95
Hexacene	$^1B_{3u}$	0.18	−0.20	−0.33	−0.54	0.16	0.42	3.09
N-phenylpyrrole	$1\,^1B_2$	0.22	0.40	−0.52	0.02	1.09	1.23	4.85
N-phenylpyrrole	$2\,^1A_1$	0.04	0.21	−0.56	−0.02	0.49	0.61	5.13
DMABN	^1B	0.44	0.38	−0.26	0.25	1.02	1.22	4.25
$H(C_2H_2)_2H$	$1\,^1B_u$	0.17	−0.01	−0.30	−0.08	0.31	0.52	5.92
$H(C_2H_2)_3H$	$1\,^1B_u$	0.13	0.14	−0.39	−0.13	0.36	0.56	4.95
$H(C_2H_2)_4H$	$1\,^1B_u$	0.04	0.01	−0.53	−0.25	0.31	0.50	4.41
$H(C_2H_2)_5H$	$1\,^1B_u$	−0.26	−0.33	−0.86	−0.57	0.03	0.21	4.27

[a]TD-DFT/def2-TZVPD, full linear response (no TDA). Positive errors indicate that the TD-DFT transition energy is larger than the benchmark value. [b]From Ref. 1.

Table S3: Vertical excitation energies and errors for linear acenes, computed using optimally tuned LRC-ωPBE/def2-TZVPD.

Molecule	Transition	Expt.[a] (eV)	TD-DFT Error (eV)[b]					ΔLRC (eV)[d]
			PBE	PBE0	HF-PBE	LRC-ω_{GDD}PBE[c]	LRC-ω_{IE}PBE[c]	
Naphthalene	^1L_a	4.66	−0.57	−0.22	0.17	−0.09	0.01	0.08
Naphthalene	^1L_b	4.13	0.14	0.42	0.91	0.45	0.40	0.05
Anthracene	^1L_a	3.60	−0.68	−0.33	0.18	−0.03	−0.11	0.06
Anthracene	^1L_b	3.64	−0.01	0.28	0.76	0.41	0.30	0.09
Tetracene	^1L_a	2.88	−0.72	−0.39	0.12	−0.07	−0.18	0.11
Tetracene	^1L_b	3.39	−0.35	0.14	0.56	0.34	0.18	0.16
Pentacene	^1L_a	2.37	−0.75	−0.43	0.05	−0.05	−0.16	0.11
Pentacene	^1L_b	3.12	−0.74	−0.04	0.51	0.41	0.21	0.20
Hexacene	^1L_a	2.02	−0.79	−0.49	−0.04	−0.03	−0.14	0.11
Hexacene	^1L_b	2.87	−0.11	−0.32	0.38	0.16	0.02	0.14
MAE[e]						0.20	0.17	0.12

[a]From Ref. 7. [b]Relative to experiment. [c]Optimal tuning, $c_{\mathrm{hfx}} = 0$. [d]Difference between LRC-ω_{GDD}PBE and LRC-ω_{IE}PBE excitation energies. [e] Mean absolute error, relative to experiment

Table S4: DFT and TD-DFT properties for the linear acenes, computed using optimally tuned LRC-ωPBE/def2-TZVPD.[a]

No. Rings	GDD tuning				IE tuning				LRC-ωPBE		
	ω_{GDD} (bohr^{-1})	$\Delta E(^1\mathrm{L}_a)^b$ (eV)	d_{rms} (Å)	KS gap (E_{h})	ω_{IE} (bohr^{-1})	$\Delta E(^1\mathrm{L}_a)^b$ (eV)	d_{rms} (Å)	KS gap (E_{h})	$\Delta E(^1\mathrm{L}_a)^b$ (eV)	d_{rms} (Å)	KS gap (E_{h})
2	0.302	4.58	3.1672	0.312	0.256	4.51	3.197	0.300	4.58	3.1681	0.312
3	0.289	3.57	3.9707	0.252	0.227	3.45	4.0411	0.237	3.59	3.9608	0.255
4	0.276	2.82	4.4754	0.214	0.207	2.70	4.5859	0.197	2.84	4.4498	0.218
5	0.267	2.32	4.9265	0.187	0.191	2.21	5.0967	0.170	2.35	4.8843	0.192
6	0.262	1.99	5.3269	0.169	0.179	1.87	5.5729	0.150	2.01	5.2702	0.174
7	0.255	1.75	5.6908	0.155	0.169	1.63	6.0201	0.136	1.76	5.6123	0.160
8	0.252	1.58	6.0090	0.145	0.162	1.45	6.4289	0.125	1.59	5.9149	0.150
9	0.248	1.45	6.2957	0.137	0.157	1.32	6.7994	0.117	1.45	6.1819	0.142

[a]These are the data used in Fig. 3. [b]TD-DFT(TDA).

Table S5: DFT and TD-DFT properties for linear acenes computed using optimally tuned LRC-ωPBE/def2-ma-SVP.[a]

No. of Rings	GDD tuning			IE tuning		
	ω_{GDD} (bohr^{-1})	$\Delta E(^1\mathrm{L}_a)^b$ (eV)	KS gap (E_{h})	ω_{IE} (bohr^{-1})	$\Delta E(^1\mathrm{L}_a)^b$ (eV)	KS gap (E_{h})
2	0.316	4.65	0.315	0.270	4.61	0.308
3	0.299	3.72	0.257	0.238	3.60	0.242
4	0.286	2.98	0.219	0.216	2.84	0.202
5	0.277	2.49	0.194	0.198	2.34	0.173
6	0.270	2.14	0.175	0.186	1.98	0.152
7	0.267	1.90	0.162	0.175	1.63	0.136
8	0.262	1.72	0.152	0.168	1.54	0.129
9	0.257	1.59	0.144	0.162	1.44	0.121
10	0.252	−0.01	0.087	0.158	1.34	0.115
11	0.250	0.02	0.087	0.127	0.26	0.074
12	0.245	0.05	0.087	0.121	0.29	0.073
15	0.238	0.06	0.086	0.107	0.33	0.070
20	0.229	0.07	0.085	0.102	0.32	0.068
40	0.212	0.11	0.080	0.098	0.31	0.066

[a]These are the data used in Fig S2. [b]TD-DFT(TDA).

Table S6: DFT and TD-DFT properties for $(PPV)_n$ oligomers computed using optimally tuned LRC-ωPBE/def2-ma-SVP.[a]

Size	GDD tuning				IE tuning				LRC-ωPBE		
(n)	ω_{GDD}	$\Delta E(S_1)$[b]	d_{rms}	KS gap	ω_{IE}	$\Delta E(S_1)$[b]	d_{rms}	KS gap	$\Delta E(S_1)$[b]	d_{rms}	KS gap
	(bohr^{-1})	(eV)	(Å)	(E_h)	(bohr^{-1})	(eV)	(Å)	(E_h)	(eV)	(Å)	(E_h)
1	0.321	5.18	2.9082	0.291	0.270	5.06	2.9536	0.334	5.13	2.9241	0.343
2	0.285	4.14	4.3247	0.273	0.214	3.99	4.5459	0.250	4.16	4.2917	0.277
3	0.268	3.58	5.1117	0.244	0.187	3.36	5.5840	0.214	3.64	5.0006	0.252
4	0.258	3.29	5.5871	0.229	0.173	3.04	6.2880	0.197	3.38	5.4009	0.239
5	0.249	3.12	5.8904	0.219	0.166	2.85	6.7351	0.187	3.23	5.6271	0.232
6	0.242	3.01	6.0869	0.213	0.162	2.73	7.0164	0.181	3.14	5.7568	0.228
7	0.237	2.93	6.2170	0.209	0.160	2.65	7.1876	0.178	3.08	5.8352	0.225
8	0.233	2.88	6.3092	0.205	0.162	2.62	7.2343	0.176	3.04	5.8852	0.223
9	0.229	2.84	6.3835	0.203	0.162	2.58	7.2885	0.175	3.01	5.9175	0.222
10	0.226	2.80	6.4399	0.201	0.166	2.57	7.2504	0.176	2.99	5.9413	0.221
11	0.223	2.78	6.4801	0.199	0.168	2.57	7.2268	0.177	2.98	5.9493	0.221

[a]These are the data used in Fig. 3. [b]TD-DFT(TDA).

Table S7: DFT and TD-DFT properties for $O_2N(Ph)_nNH_2$ oligomers, computed using optimally tuned LRC-ωPBE/def2-ma-SVP.[a]

Size	GDD tuning				IE tuning				LRC-ωPBE		
(n)	ω_{GDD}	$\Delta E(S_1)$[b]	d_{rms}	KS gap	ω_{IE}	$\Delta E(S_1)$[b]	d_{rms}	KS gap	$\Delta E(S_1)$[b]	d_{rms}	KS gap
	(bohr^{-1})	(eV)	(Å)	(E_h)	(bohr^{-1})	(eV)	(Å)	(E_h)	(eV)	(Å)	(E_h)
1	0.315	3.9248	2.3415	0.2962	0.248	3.8349	2.4354	0.2747	3.9047	2.3587	0.2921
2	0.290	3.8454	2.4303	0.2535	0.222	3.7498	2.5863	0.2307	3.8591	2.4142	0.2562
3	0.278	3.8271	2.4008	0.2398	0.217	3.7385	2.6224	0.2177	3.8576	2.3625	0.2461
4	0.269	3.8139	2.4003	0.2332	0.216	3.7367	2.5342	0.2134	3.8571	2.3500	0.2424
5	0.259	3.7992	2.4201	0.2251	0.215	3.7344	2.5325	0.2083	3.8566	2.3495	0.2375
6	0.253	3.7887	2.4281	0.2216	0.214	3.7308	2.5274	0.2063	3.8547	2.3473	0.2359
7	0.248	3.7825	2.4425	0.2207	0.215	3.7333	2.5296	0.2077	3.8558	2.3498	0.2370
8	0.243	3.7764	2.4527	0.2187	0.215	3.7345	2.5275	0.2074	3.8571	2.3491	0.2367

[a]These are the data used in Fig. 3. [b]TD-DFT(TDA).

Table S8: TD-DFT Results for open-shell and exotic molecules using the LRC-ωPBEh functional.[a]

Transition	ω (bohr^{-1})		Error (eV)[b]	
	GDD	IE	GDD	IE
BeF ($^2\Pi$)	0.392	0.457	0.07	0.07
BH_2 ($^2B_1$)	0.407	0.427	0.11	0.11
CN ($^2\Pi$)	0.485	—[c]	−0.28	—[c]
HCF ($^1A''$)	0.466	0.401	−0.09	−0.13
NH_2 ($^2A_1$)	0.536	0.566	−0.09	−0.09
NO ($^2\Sigma^+$)	0.509	0.515	−0.11	−0.11
OH ($^2\Sigma^+$)	0.443	1.490	0.12	0.68
NCO ($^2\Sigma^+$)	0.448	1.426	0.49	0.86
MAE			0.10	0.29

[a] LRC-ωPBEh/def2-TZVPD. [b] With respect to theoretical best estimates from Ref. 8. Positive errors indicate that the TD-DFT transition energy is larger than the benchmark. [c] IE tuning is omitted because $\omega_{IE} \to \infty$.

FIGURES

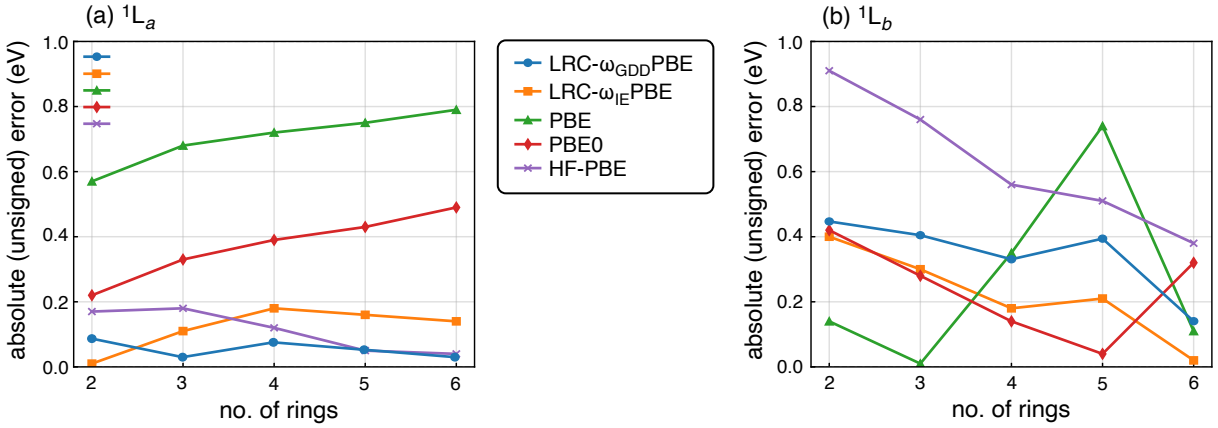

Figure S1: Mean absolute errors in TD-DFT(TDA)/def2-TZVPD calculations with various functionals, for (a) the ^1L_a and (b) the ^1L_b state of the linear acenes, naphthalene through hexacene.

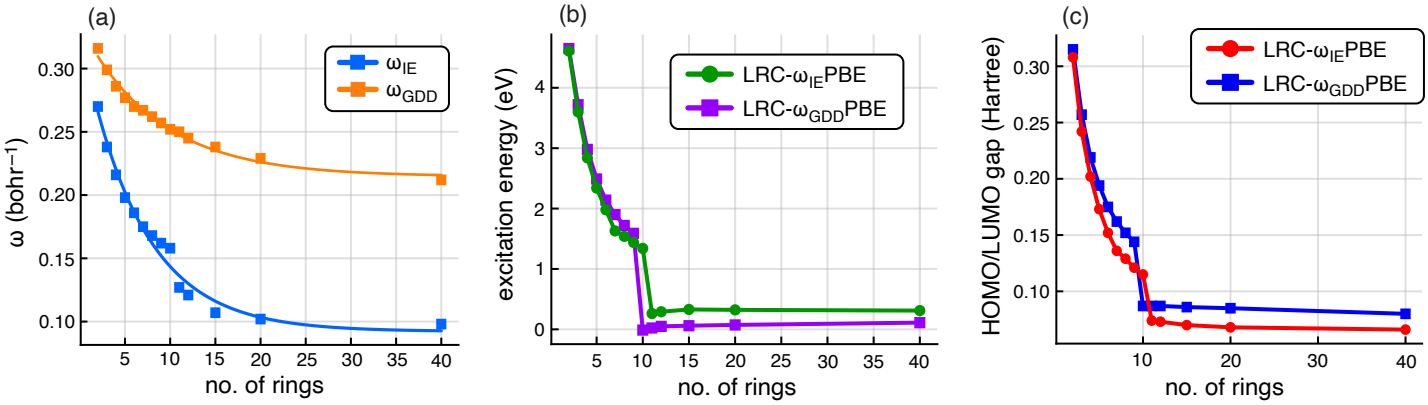

Figure S2: Variation of linear acene properties versus molecular size: (a) tuned ω values, (b) S_1 excitation energies, and (c) HOMO/LUMO gaps. DFT and TD-DFT(TDA) calculations performed using the def2-ma-SVP basis set.

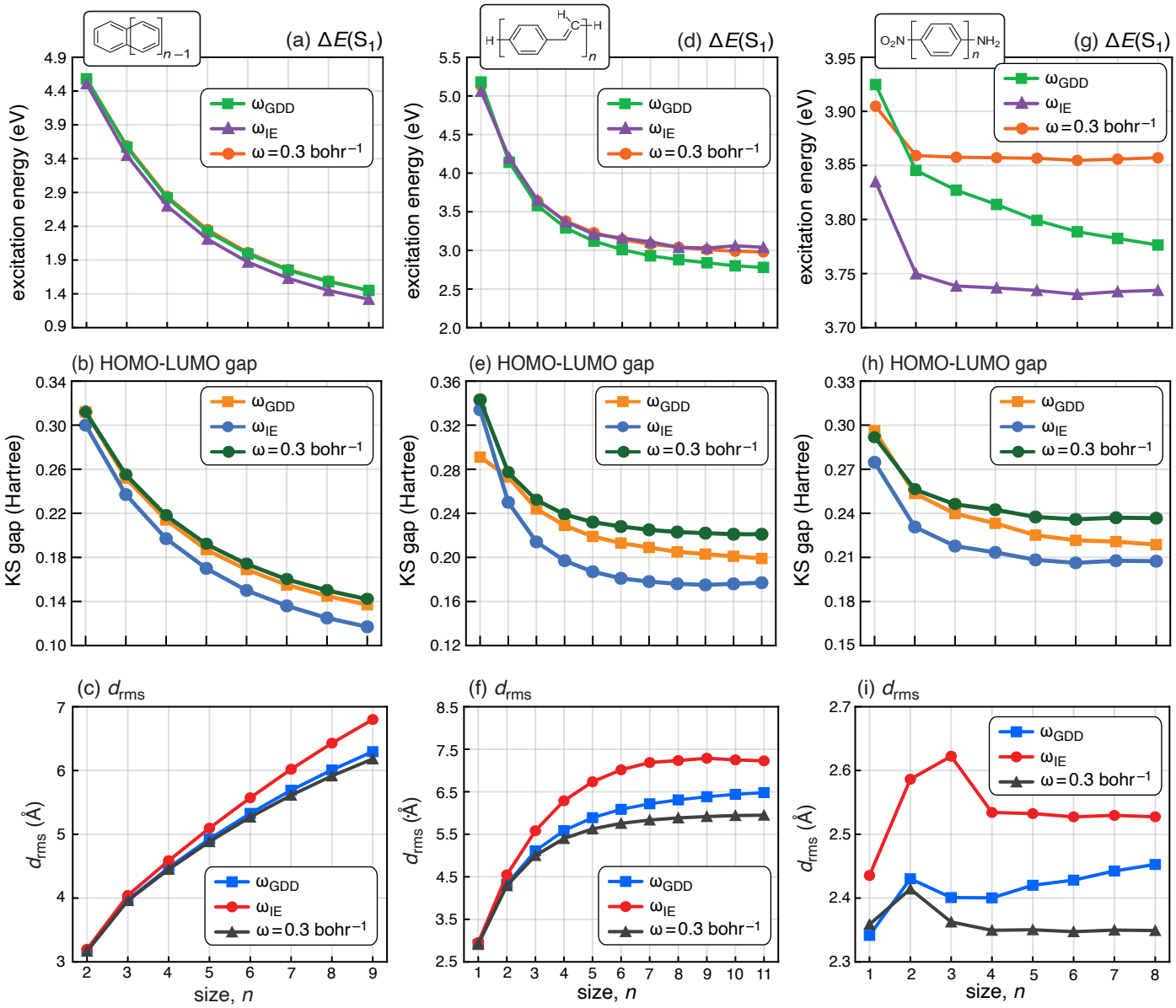

Figure S3: TD-DFT results for conjugated polymers using tuned LRC-ωPBE functionals alongside LRC-ωPBE with fixed $\omega = 0.3$ bohr^{-1}. (a) TD-DFT(TDA) excitation energies for the S_1 state, (b) HOMO-LUMO gaps, and (c) exciton size (d_{rms}) for linear acene molecules. (d) Excitation energies $\Delta E(S_1)$, (e) HOMO-LUMO gaps, and (f) d_{rms} for $(\mathrm{PPV})_n$ oligomers. (g) Excitation energies $\Delta E(S_1)$, (h) HOMO-LUMO gaps, and (i) d_{rms} for $O_2N(Ph)_nNH_2$. Acene calculations were performed using the def2-TZVPD basis set and other calculations used def2-ma-SVP.

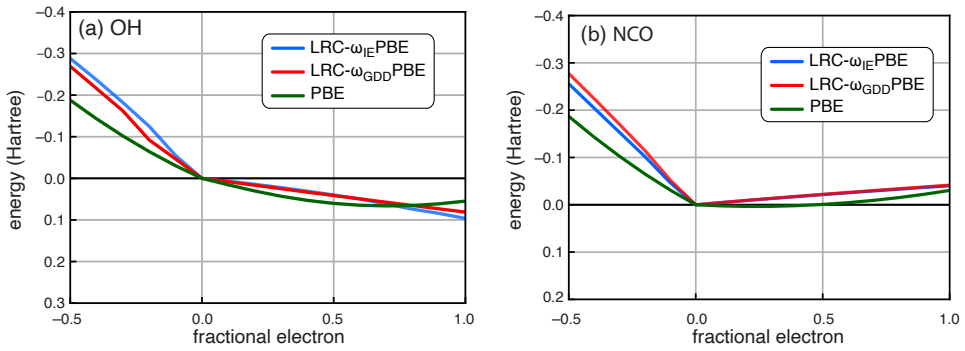

Figure S4: Variation of total energy with respect to fractional electron added, for two open shell systems. All calculations were performed using the def2-TZVPD basis set.

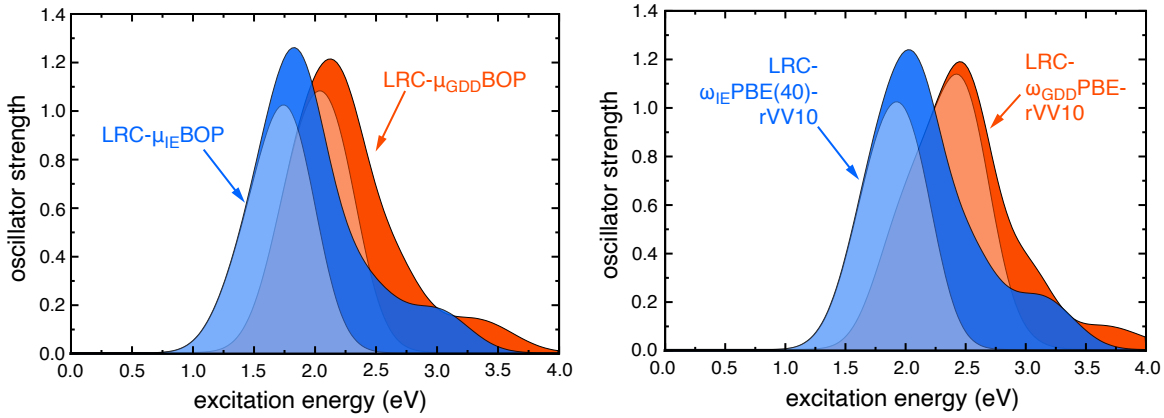

Figure S5: Simulated absorption spectra of e^-(aq) using three QM/MM snapshots with 68–71 DFT water molecules. Vertical transition energies computed using TD-DFT(TDA)/6-31++G* were broadened by 0.2 eV Gaussians and weighted by oscillator strength. Spectra in solid colors include 15 excited states and the translucent spectra on top illustrate the result from just the first three excited states. The procedure is the same as that used with the LRC-ωPBE functional in Fig. 4, but the LRC-μBOP and LRC-ωPBE(40)-rVV10 functionals is used here, as in previous studies of the e^-(aq) absorption spectrum.[2–5] Additional data points would smooth out the blue tail, as in Fig. 4 that uses seven QM/MM snapshots.